12

Iodine Quantification Based on Rest / Stress Perfusion Dual Energy CT to Differentiate Ischemic, Infarcted and Normal Myocardium

Marly van Assen, Francesco Lavra, U. Joseph Schoepf, Brian E. Jacob, Baxter T. Williams, Zachary M. Thompson, Akos Varga-Szemes, Balazs Ruzsics, Matthijs Oudkerk, Rozemarijn Vliegenthart, Carlo N. De Cecco

Published EJR 2019

ABSTRACT

Background: The aim of this study was to assess the potential of rest-stress DECT iodine quantification to discriminate between normal, ischemic, and infarcted myocardium.

Methods: Patients who underwent rest-stress DECT on a 2nd generation dual-source system and cardiac magnetic resonance (CMR) were retrospectively included from a prospective study cohort. CMR was performed to identify ischemic and infarcted myocardium and categorize patients into ischemic, infarcted, and control groups. Controls were analyzed on a per-slice and per-segment basis. Regions of interest (ROIs) were placed in ischemic and infarcted areas based on CMR. Additionally, ROIs were placed in the septal area to assess normal and remote myocardium.

Results: We included 42 patients: 10 ischemic, 17 infarcted, and 15 controls. Iodine concentrations showed no significant between segments in controls. Iodine concentrations for normal myocardium increased significantly from rest to stress (median 3.7mg/mL (interquartile range 3.5-3.9) vs. 4.5mg/mL (4.3-4.9)) ($p<0.001$). Iodine concentrations in diseased myocardium were significantly lower than in normal myocardium; 1.3mg/mL (0.9-1.8) and 0.6mg/mL (0.4-0.8) at rest and stress in ischemic myocardium, and 0.3mg/mL (0.3-0.5) and 0.5mg/mL (0.5-0.7) at rest and stress in infarcted myocardium ($p<0.005$ and $p<0.001$). At rest only, iodine concentrations were significantly lower in infarcted vs. ischemic myocardium ($p<0.001$). The optimal threshold for differentiating diseased from normal myocardium was 2.5mg/mL and 2.1mg/mL for rest and stress (AUC 1.00). To discriminate ischemic from infarcted myocardium, the optimal threshold was 1.0mg/ml (AUC 0.944) at rest.

Conclusion: DECT iodine concentration from rest-stress imaging can potentially differentiate between normal, ischemic, and infarcted myocardium.

INTRODUCTION

Dual-energy CT (DECT), which uses both high- and low-energy x-ray photons, allows for the quantification of materials and tissues based on unique attenuation values at different energy levels(1,2). For this reason, DECT enables the assessment of iodine concentrations in the myocardium(3–6). A body of evidence has validated the direct relationship between iodine distribution in the myocardium and myocardial blood flow, suggesting that myocardial iodine concentration may serve as a potential quantitative imaging biomarker to assess myocardial perfusion(1–4,7).

To date, the majority of cardiac DECT studies have focused on the evaluation of iodine maps for the detection of myocardial perfusion defects; however, most investigations lack quantitative measurements of iodine concentration(2,8–12). Several phantom studies have reported that DECT can accurately measure iodine concentrations(3,6,7). A previous study using stress-only DECT showed that a difference in iodine concentration was present between normal, ischemic, and infarcted segments when using cardiac magnetic resonance (CMR) perfusion imaging and late gadolinium enhancement (LGE) studies as reference standards (13). In particular, diseased segments had significantly lower iodine concentrations than normal segments. Additionally, ischemic segments had higher iodine concentrations relative to infarcted segments. However, a reliable threshold to discriminate between ischemic and infarcted segments could not be determined using stress-only DECT iodine concentrations. Comparing values at both rest and stress may improve tissue characterization by providing incremental information. Furthermore, DECT acquisitions at rest may provide information about the hemodynamic significance of CAD based on iodine quantification without the need for a stress acquisition.

Thus, the purpose of this study was to assess the potential of rest-stress DECT iodine quantification to differentiate between normal, ischemic, and infarcted myocardium using CMR as the reference standard.

METHODS

For this study, patients were retrospectively selected from a prospective study cohort. This prospective, single-center study was approved by our local Institutional Review Board and conducted in compliance with the Health Insurance Portability and Accountability Act. All patients provided written informed consent.

Population

Our investigation included 46 patients with suspected CAD who had undergone a rest-stress cardiac DECT perfusion study between 2008 and 2012. All patients underwent stress CMR perfusion imaging for the evaluation of CAD. Patients with missing rest or stress DECT data, or poor image quality were excluded from the study. Patients were assigned to their respective cohorts based on stress CMR. CMR was used as the gold standard, considering the relatively low accuracy and spectral resolution of SPECT imaging(14,15).

Patients without delayed enhancement or defects on perfusion series were assigned to the control group. Patients with a clear defect on the CMR perfusion series but without delayed enhancement on LGE were assigned to the ischemic group. Patients with clear delayed enhancement on LGE series were assigned to the infarcted group. Patients with perfusion defects on CMR with less than 15% transmurality were excluded due to the difficulty of accurately analyzing ROI-based data on both MRI and DECT images. All scans were evaluated by two board-certified radiologists with 11 and 20 years of experience in cardiovascular imaging, respectively. The two radiologists were blinded to all clinical and other imaging data during the analysis. A minimum of four weeks was maintained between the reading of CMR and DECT data to reduce potential recall bias. CMR acquisitions were used as the reference standard.

Imaging protocols

All patients underwent rest/stress CMR and DECT perfusion. DECT and CMR imaging procedures were performed on the same day.

DECT

All DECT examinations were acquired using a second-generation dual-source CT system (Definition Flash; Siemens Healthineers, Forchheim, Germany) in dual energy mode. DECT examinations were performed at rest and during maximal hyperemia (**Figure 1A**). All scans were performed using retrospective ECG gating and ECG-dependent tube current modulation. Additional acquisition parameters included: 2 x 64 x 0.6 mm (rest) and 2 x 64 x 1.5 mm (stress) detector collimation with z-flying focal spot technique, 280-msec gantry rotation time, heart rate adaptive pitch of 0.2–0.43, and a temporal resolution of 140 msec. Tube A was operated with 140 mAs per rotation at 140 kVp using an additional tin filter. Tube B was operated with 165 mAs per rotation at 100 kVp. Scans were acquired in the craniocaudal direction.

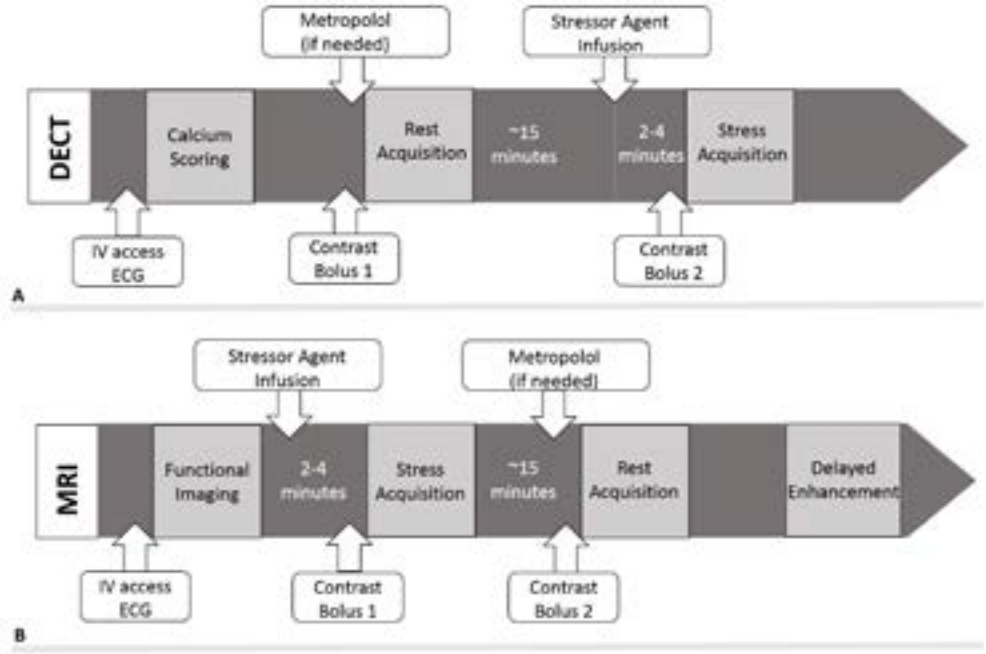

Figure 1: A) DECT and B) CMR acquisition protocols. The following were administered: adenosine (Adenoscan; Astellas, Northbrook, Ill), regadenoson (Lexiscan; Astellas, Northbrook, Ill), metoprolol as metoprolol tartrate (Lopressor; Novartis, East Hanover, NJ).

Rest imaging was performed first. Metoprolol (Lopressor; Novartis, East Hanover, NJ) was administered to patients with heart rates > 65 beats per minute. For both stress and rest examinations, 75 mL of 370 mgI/mL iopromide (Ultravist; Bayer Healthcare, Wayne, NJ) was intravenously administered at an injection rate of 6 mL/s. Contrast media administration was followed by a 50 mL saline flush bolus at the same injection rate.

Stress perfusion imaging was performed 3-4 minutes into continuous adenosine infusion (140 µg/kg/min) (Adenoscan; Astellas, Northbrook, Ill) or after a single regadenoson injection (0.4 mg/5mL) (Lexiscan; Astellas, Northbrook, Ill).

To ensure optimal timing for scan acquisition, the bolus-tracking technique was used with a 70 HU threshold in the descending thoracic aorta and an additional 2 second delay. Data were reconstructed in the diastolic phase (60-75%) with a section thickness of 3 mm for both rest and stress acquisitions.

CMR

All CMR examinations were acquired on a 1.5T system (Siemens Magnetom Avanto, Siemens Healthineers, Erlangen, Germany). In total, 0.1 mmol/kg (0.2 ml/kg)

of gadolinium-based contrast material (MultiHance; Bracco, Milan, Italy) was intravenously administered in two separate injections, prior to both stress and rest perfusion (0.1 ml/kg each), at an injection rate of 4 ml/s and was followed by a 20 ml saline flush bolus.

First-pass perfusion imaging was performed during maximal hyperemia and rest **(Figure 1B)** using a T1-weighted fast low-angle single-shot gradient-echo pulse sequence with the following typical parameters: slice thickness 8 mm, acquisition matrix 144×76, in-plane resolution 2.63×2.63 mm^2, echo/repetition time (TE/TR) 1.0/2.2 ms, flip angle 10°, saturation recovery time 100 ms, generalized auto-calibrating partially parallel acquisition (GRAPPA) with acceleration factor 2, and Cartesian readout. Stress perfusion was performed first, 2-4 minutes after continuous adenosine infusion (140 µg/kg/min) or a single regadenoson injection (0.4 mg/5mL). Rest perfusion series were acquired, at minimum, 15 min after regadenoson/adenosine administration was discontinued (adenosine) or reversed with aminophylline (regadenoson).

LGE imaging was performed 15 min after completion of the rest perfusion. LGE images were acquired over three slices, with slice positions kept as consistent with the perfusion slices as possible. An inversion recovery steady-state free-precession pulse sequence was used with the following typical parameters: slice thickness 8 mm, acquisition matrix 192×104, in-plane resolution 1.98×1.98 mm^2, TE/TR 1.1/2.6 ms, readout bandwidth 965 Hz/pixel, flip angle 50°, generalized auto-calibrating partially parallel acquisition (GRAPPA) with acceleration factor 2, and Cartesian readout. Inversion time was adjusted to null the signal in the normal myocardium. Data were reconstructed in a magnitude-based fashion.

Image analysis

DECT iodine maps were analyzed for control patients on a per-segment basis based on the AHA 17-segment model, with the 17th segment excluded from analysis. Image quality evaluation was performed on a per-segment and per-patient basis. All scans were assessed for overall image quality and were scored by an experienced radiologist (CNDC) using a four-point Likert scale (1-4), where 1 represents poor image quality and 4 represents excellent image quality. All segments underwent strict and extensive quality control assessment; segments with poor quality were excluded.

In the control group, iodine concentrations were derived from the iodine quantification maps generated at both rest and stress on a per-segment and per-slice basis, including the basal, mid-ventricular, and apical slices. Slices were determined by dividing the left ventricle into equal thirds in a direction perpendicular to the long-axis of the heart.

Additionally, to compare normal, ischemic, and infarcted areas of the myocardium, regions of interest (ROI) were drawn on the iodine maps. The iodine concentration of normal myocardium in control patients and remote myocardium in patients with CAD was measured using a single ROI in the septum (mid-ventricular slice) with a minimum area of 1 cm^2. In patients with CAD, mean iodine concentration of ischemic myocardium was measured by placing an additional ROI in an area corresponding to the reversible perfusion defect visualized on first-pass CMR. Infarcted myocardium was defined by placing a ROI where an area of infarction was visualized on LGE images. If the ischemic or infarcted region was located in the septum, the ROI for remote myocardium was placed in a different area without perfusion defect. Potential artifacts were carefully avoided during ROI placement.

To avoid partial volume contamination from the left ventricular blood pool, all infarct ROIs were placed at the infarct core, away from the endocardial and epicardial borders. Remote myocardial ROIs on the DECT images were placed in areas without evidence of first-pass perfusion defects, regional wall motion abnormalities, or LGE. A ROI was also placed in the left ventricular blood pool as a reference. A second reader repeated all ROI-based measurements in order to evaluate inter-observer variability. Measurements from the first reader were used for all other evaluations to simulate a clinical workflow.

Statistical analysis

Continuous values were presented as mean ± standard deviation (SD) or as median with interquartile ranges (IQR). Normality of data distribution was assessed using a Shapiro-Wilks test. Categorical data were presented as a number with the corresponding percentage. A Mann Whitney-U or Kruskal-Wallis test was used to compare non-normally distributed data between groups. The Wilcoxon test was used for paired data to compare rest/stress and remote/diseased myocardium iodine concentrations within groups. Intraclass correlation coefficients (ICC) were calculated to assess inter-observer variability. Receiver operator characteristic (ROC) curves and corresponding area under the curve (AUC) calculations were used to determine iodine concentration thresholds to discriminate between normal/diseased myocardium and subsequently ischemic/infarcted myocardium. All statistical analyses were performed using SPSS Statistics 23 (IBM Corporation, USA). A p-value<0.05 was considered statistically significant.

RESULTS

Baseline patient characteristics and results are presented in **Table 1**. After excluding patients with poor image quality (n=3), a total of 42 patients were included: 10 with

ischemic myocardium, 17 with infarcted myocardium, and 15 control patients. An overview of the inclusion process and corresponding measurements is depicted in **Figure 2**. Median image quality was rated a 3 (IQR 2-4). A significant increase in heart rate was observed between rest and stress DECT imaging (p<0.009) in all three groups. There was no significant difference in body mass index between groups. The mean radiation dose per patient was 10.7 ±4.5 mSv.

A total of 424 segments were included in the analysis, while 56 were excluded due to extensive artifacts or because they were outside the dual energy field of view.

Table1: Patient Characteristics

	Controls N=15	**Ischemic N=10**	**Infarcted N=17**
Male, n	9 (60%)	10 (100%)	16 (94%)
Age, years	63.2 (57.1-71.1)	64.0 (59.3-74.5)	64.2 (54.3-70.8)
BMI, kg/m^2	31.4 (26.1-33.9)	29.4 (24.0-32.3)	28.2 (25.0-31.3)
Heart rate rest, beats per minute	63 (55-77)	59 (54-68)	66 (61-74)
Heart rate stress, beats per minute	84 (67-96)	79 (64-85)	78 (73-92)
Cardiovascular Risk factors			
Diabetes	8 (53%)	2 (18%)	3 (17%)
Hypertension	13 (87%)	5 (45%)	13 (76%)
Current smoker	3 (20%)	8* (72%)	2 (12%)
Hyperlipidemia	7 (47%)	8* (72%)	11 (65%)

Values are given as median (IQR) or n (%).).* indicates significant difference compared to the control group.

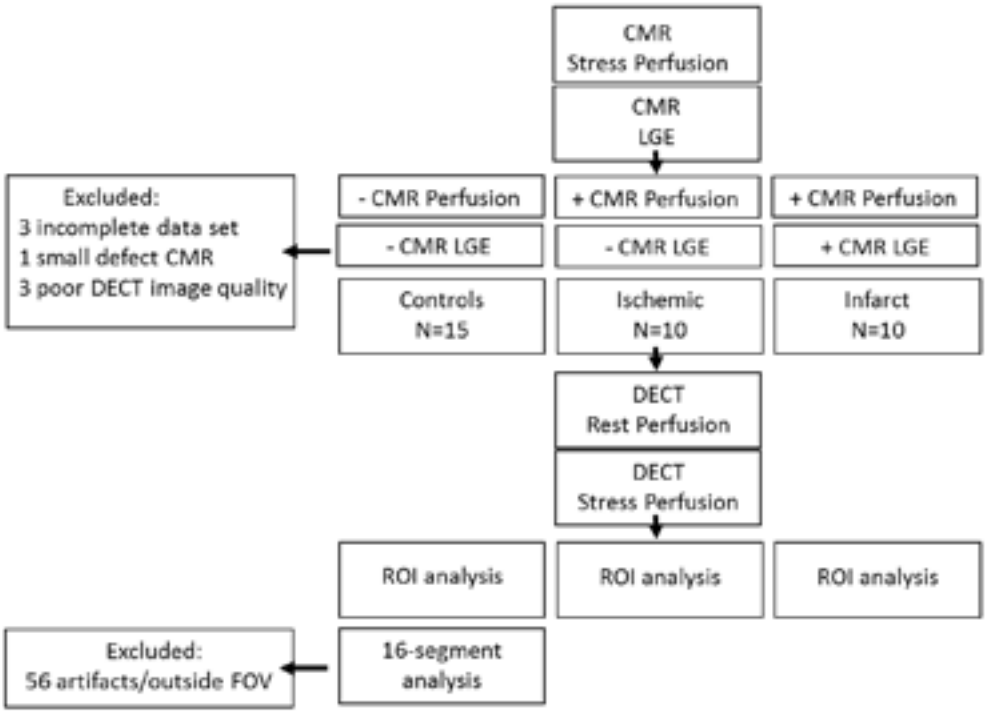

Figure 2: In total, 49 patients who underwent CMR perfusion and LGE imaging as well as rest/stress DECT imaging were included. Of those 49 patients, 7 were excluded, resulting in a total of 42 patients for analysis. A total of 54 individual segments were excluded from per-segment analysis in the control group due to poor image quality or because the segment was outside the DECT field of view.

Iodine Concentration in Normal Controls

Iodine concentrations in each segment were not significantly different at rest (p=0.650) or stress (p=0.835). Additionally, iodine concentrations in each slice were not significantly different for rest (p=0.235) or stress (p=0.416) imaging **(Figure 3)**. The median iodine concentration for normal myocardium at rest and stress was 3.7 mg/mL (IQR 3.5-3.9) and 4.5 mg/mL (IQR 4.3-4.9), respectively (p<0.001).

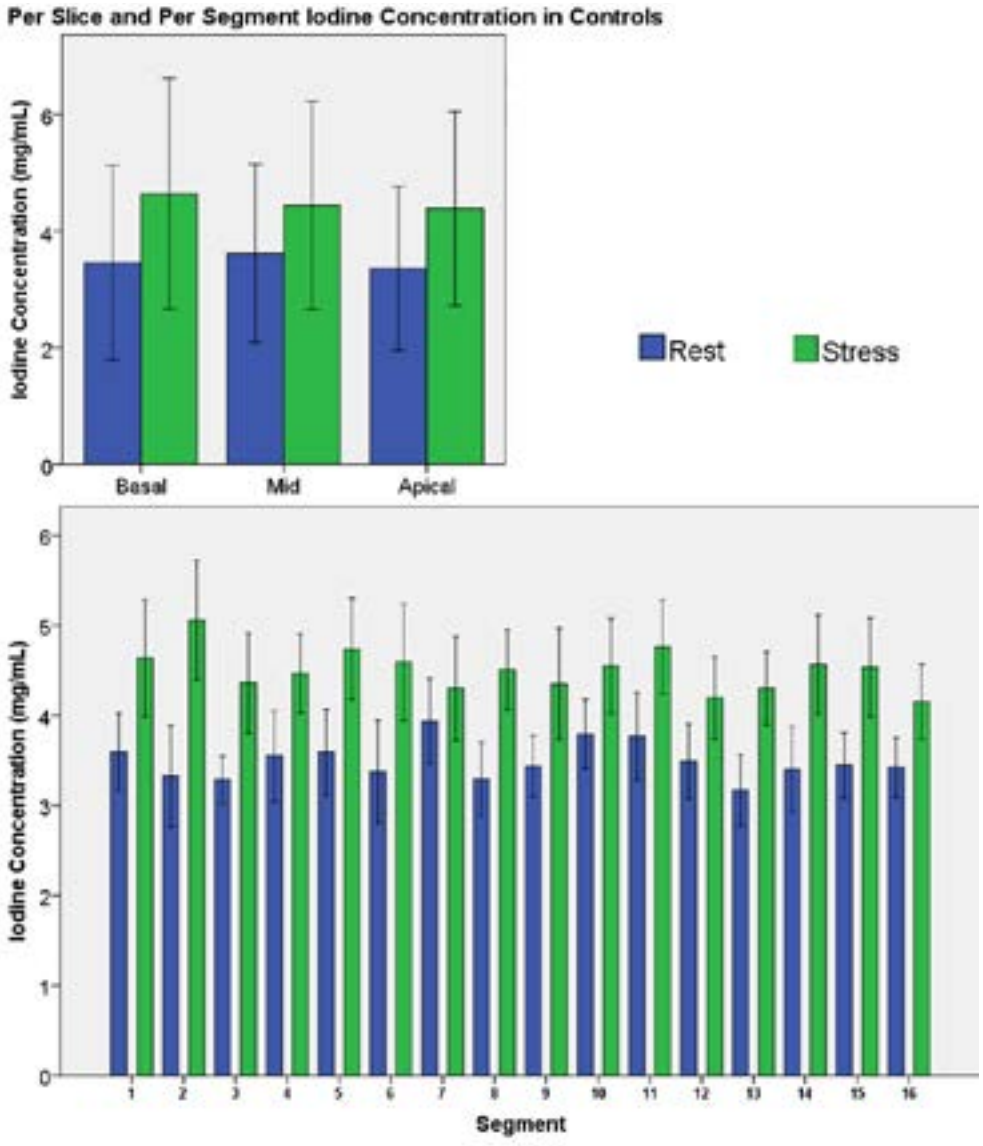

Figure 3: Iodine concentrations showed no significant variations between basal, midventricular, and apical slices at rest or stress. Analysis according to AHA 16-segment model demonstrates that iodine concentrations showed no significant differences between segments at rest and stress. Iodine concentrations during stress were higher than during rest.

Iodine Concentration in Ischemic and Infarcted Patients

Table 2 shows iodine concentrations for the three groups. Our data demonstrated good agreement with ischemic and infarcted areas on CMR perfusion imaging (**Figure 4**).

The median iodine concentration at rest in the remote myocardium of the ischemic and infarcted groups was 3.2 mg/mL (IQR 2.9-3.6) and 3.5 mg/mL (IQR 3.4-4.0), respectively. These values increased significantly during stress to 4.7 mg/mL (IQR 4.2-4.8) and 5.1 mg/mL (IQR 4.2-5.4) for the ischemic and infarcted group, respectively ($p<0.005$ and <0.001). All values are presented in **Table 2.**

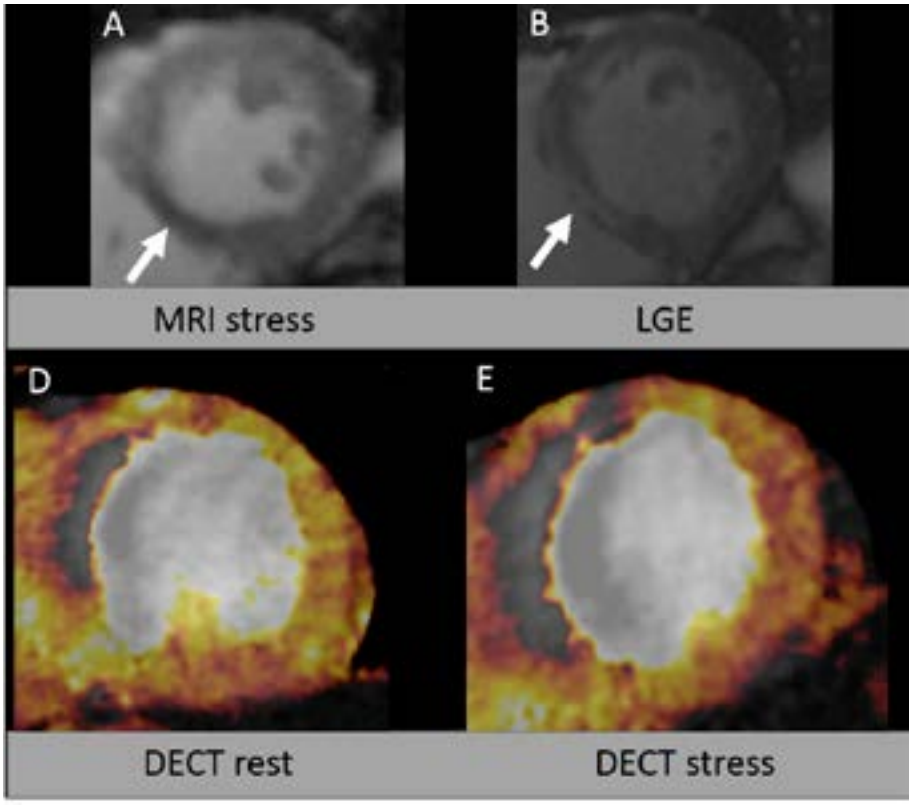

Figure 4: A 67-year-old man with known CAD. Stress perfusion CMR images show a perfusion defect in both rest and stress acquisitions in the inferior-septal wall (see arrows). The same defect is seen on the DECT iodine maps. The defect appears more pronounced during stress, indicating some level of reversibility (peri-infarct ischemia) at the borders of the infarct.

The iodine concentration at rest in the remote myocardium of the ischemic group was significantly lower than the normal myocardium of control patients ($p<0.005$); however, this was not observed during stress ($p = 0.911$). Iodine concentration of remote myocardium in the infarcted group showed no significant difference compared to the normal myocardium of the control group at both rest and stress ($p=0.455$ and 0.370, respectively). There was no significant difference in iodine concentration of

remote myocardium between the ischemic and infarcted groups at both rest and stress (p=0.052 and 0.155, respectively).

At rest and stress, the iodine concentration of ischemic myocardium was 1.3 mg/mL (IQR 0.9-1.8) and 0.6 mg/mL (IQR 0.4-0.8), respectively (p<0.007). The iodine concentration of infarcted myocardium showed a significant increase between rest (median 0.3 mg/mL (IQR 0.3-0.5)) and stress (median 0.5 mg/mL (IQR 0.5-0.7)) (p<0.001).

Table 2: Iodine Concentration in Normal/Remote and Diseased Myocardium

	Normal/Remote myocardium		**Diseased myocardium**		
Status	Iodine [] (mg/mL) Rest	Iodine [] (mg/mL) Stress	Iodine [] (mg/mL) Rest	Iodine [] (mg/mL) Stress	p-value
Control	3.7 (3.5-3.9)	4.5 (4.3-4.9)	-	-	p=0.001
n =15					
Ischemic n=10	3.2 (2.9-3.6)	4.7 (4.2-4.8)	1.3* (0.9-1.8)	0.6*(0.4-0.8)	p<0.001 p=0.007
Infarcted n=17	3.5 (3.4-4.0)	5.1 (4.2-5.4)	0.3* (0.3-0.5)	0.5* (0.5-0.7)	p<0.001 p<0.001

Values are given as median (IQR).* indicates significant difference compared to the control group. A p-value<0.05 is considered statistically different.

The iodine concentrations of ischemic and infarcted myocardium were significantly lower than concentrations of remote myocardium at both rest and stress (p<0.005 and p<0.001, respectively) **(Table 2)**.

At rest, the iodine concentration in ischemic myocardium was significantly higher than the concentration in infarcted myocardium (p<0.001); however, the concentrations were similar during stress imaging (p=0.749).

Figure 5 represents image examples from patients in the control, ischemic and infarct groups.

Iodine measurement variability and accuracy

Intraclass correlation coefficients (ICC) were calculated at both rest and stress for the three different groups. At rest, the ICC was 0.84, 0.84, and 0.82 in normal, ischemic, and infarcted myocardium, respectively. During stress imaging, the ICC was 0.89, 0.96, and 0.87 in normal, ischemic, and infarcted myocardium, respectively.

Multiple thresholds were determined based on the ROC curves. The optimal threshold for discriminating diseased myocardium, either ischemic or infarcted, from normal myocardium was an iodine concentration of 2.5 mg/mL at rest and 2.1 mg/mL during stress, with a corresponding AUC of 1. For discriminating between ischemic and infarcted myocardium, the optimal threshold was an iodine concentration of 1.00 mg/mL at rest, with a corresponding AUC of 0.944, sensitivity of 80%, and specificity of 100%. Notably, an optimal threshold could not be determined during stress acquisitions, as the AUC was only 0.538 (**Figure 6**).

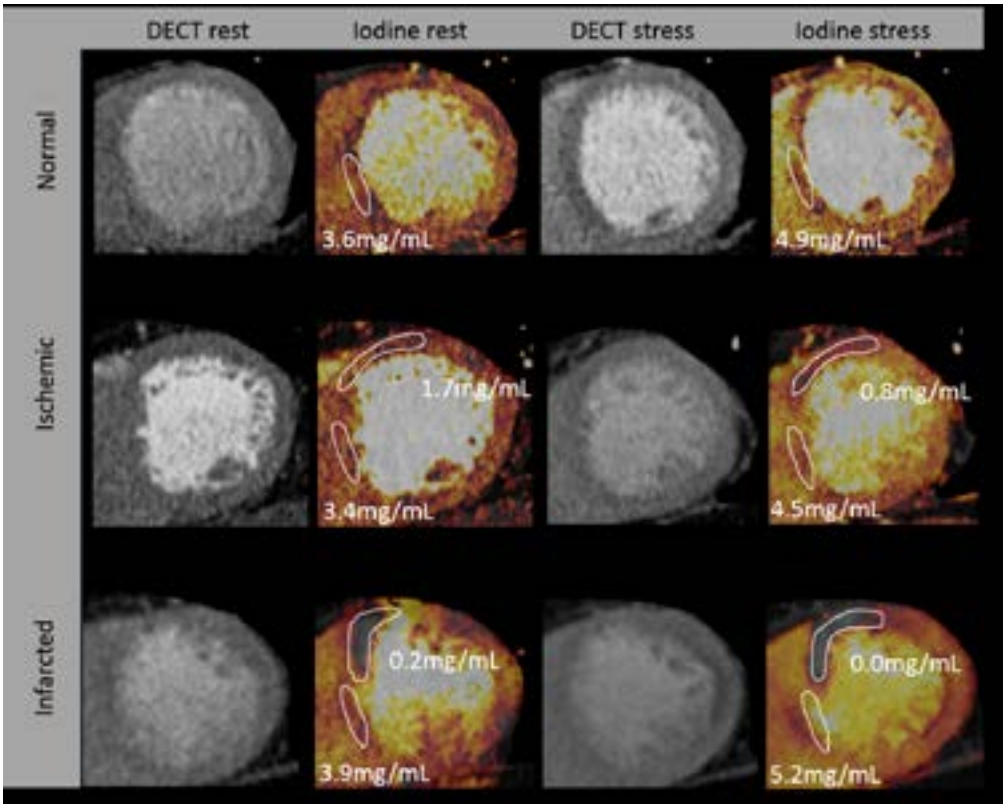

Figure 5: Examples of DECT images and iodine maps of 3 patients. The upper row shows a control patient without ischemic or infarcted myocardium, the middle row shows a patient from the ischemic group, and the bottom row shows a patient from the infarcted group. ROIs and corresponding iodine concentrations are shown in normal/remote myocardium and diseased myocardium.

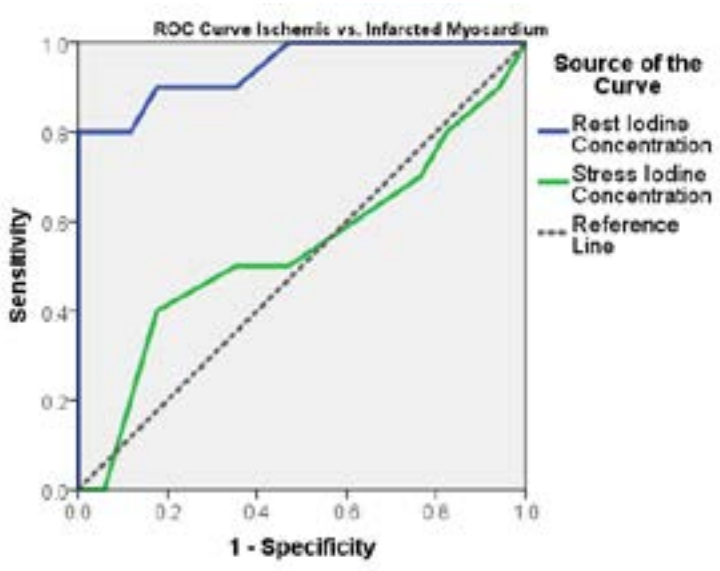

Figure 6: ROC curve representing the diagnostic performance of iodine quantification to discriminate between ischemic and infarcted myocardium. At rest, the optimal threshold was determined to be 0.95 mg/mL, with an AUC of 0.944. An iodine threshold could not be determined in the stress acquisitions due to the AUC of 0.538.

DISCUSSION

In this study, our results indicated the potential of rest and stress DECT iodine quantification to discriminate between normal, ischemic, and infarcted myocardium. Specifically, iodine concentration thresholds were determined for both rest (2.5 mg/mL) and stress (2.1 mg/mL) acquisitions and concentrations were significantly lower in diseased myocardium than in normal myocardium.

In cardiac imaging, DECT offers the potential to assess CAD on a morphological and functional basis using a single modality. With the capacity to quantify iodine concentration, DECT could join dynamic CT perfusion as a quantitative technique to analyze myocardial perfusion. Yet, DECT perfusion is a static method and greatly depends on acquisition timing, whereas dynamic CT perfusion offers the ability to visualize the entire process of contrast inflow and outflow.

Our investigation did not consider the assessment of delayed DECT acquisitions due to the results of the study by Meinel et al., which determined that a rest/stress acquisition is optimal (AUC 0.98) for the assessment of perfusion deficits, and a delayed acquisition adds little value (AUC 0.98) (15). Furthermore, our study utilized ROI-based analysis

rather than per-segment analysis. Although another previous study reported higher iodine concentrations in normal and diseased myocardium using per-segment analysis, our methodology ensures that only diseased myocardium is included in the iodine concentration calculations, effectively preventing concentration values of surrounding normal myocardium from being included in the analysis and perhaps contributing to a lower, more accurate value (13). Despite differences between the methodologies, both previous studies suggested that it was not possible to discriminate between ischemic and infarcted myocardium using stress-only acquisitions (AUC 0.538 and 0.651, respectively). In our study, we demonstrated that iodine concentrations of ischemic myocardium at rest were significantly higher compared to infarcted myocardium ($p<0.001$) and established an optimal threshold of 1.00 mg/mL (AUC 0.944) for discriminating between the two.

The iodine concentrations in normal myocardium of the control group were 3.7 mg/mL and 4.5 mg/mL at rest and stress, respectively. Pelgrim *et al.*, Koonce *et al.* and Kim et al. previously determined the accuracy of DECT to measure iodine concentration in a phantom study [3, 7, 16]. Yet, these studies indicated that varying DECT systems did not affect the iodine concentration error and used relatively higher concentrations of iodine compared to the clinical values of the current investigation. Notably, lower iodine concentrations (0-5 mg/mL) pronounced the concentration error more in comparison to intermediate concentrations. Thus, further investigations should focus on testing the accuracy of DECT for the *in-vivo* quantification of lower iodine concentrations with smaller increments.

In CMR, CT, and SPECT perfusion, a combination of both rest and stress acquisitions is used to discriminate between reversible (ischemic) and fixed (infarct) defects. In contrast to these methods, DECT perfusion shows decreased iodine concentrations in ischemic myocardium not only during stress acquisitions, but also at rest (4,15,17–19). However, as is true with traditional perfusion methods, we still see a decrease in iodine concentration from rest to stress, which is characteristic of reversible defects. Although the ischemic group was relatively small in number (n=10), these results indicate that with the use of DECT, it may be possible to identify hibernating myocardium using a rest acquisition. Notably, the iodine concentrations from the rest acquisitions show a higher variability than the iodine concentrations in other myocardial categories. Therefore, it is possible that this increased variability is correlated to the stenosis severity of the supplying vessel.

Demonstrated by the results of our investigation, the notion that iodine concentrations of remote myocardium in ischemic patients is lower than iodine concentrations of normal myocardium in the control group may provide novel insight into disease

characteristics of the remote myocardium. The CMR parameter, T1 mapping, can potentially be used for tissue characterization in CAD patients. A proof of concept study by Liu et al. showed that remote myocardium demonstrated blunted T1 reactivity (20). Previous studies using PET perfusion also show lower myocardial blood flow values in remote myocardium compared to myocardium in healthy controls, but only during stress imaging (21,22). The lower perfusion values in remote myocardium may be a result of maximal compensatory coronary microvascular vasodilatation or maximal capillary recruitment to compensate for the loss of blood flow caused by significant stenosis (20,23).

Limitations

There are several limitations beyond the retrospective nature of the current investigation that deserve special mention. First, the study has a relatively small number of patients included, especially in the ischemic group (n=10). The limited number of patients in the ischemic group may have caused the absence of a significant difference in iodine concentration between ischemic and infarcted myocardium during stress acquisitions. Second, the use of imaging examinations as the reference standard rather than an invasive technique, such as invasive coronary angiography with corresponding fractional flow reserve measurement, represents a study limitation. Specifically, the use of an invasive reference standard would allow for a better approximation of the location of the myocardial defects and for analysis of stenosis severity. Lastly, only patients with suspected or known CAD were included. Thus, patient selection bias may impact the interpretation of CMR perfusion and viability imaging.

This study serves to elucidate the potential use of rest-stress DECT iodine quantification for the differentiation of myocardial tissue. Future validation of this application will rely on large cohort studies to systematically investigate potential differences caused by age, gender, or cardiovascular risk factors and is especially important when considering differences between normal and remote myocardium. Furthermore, the effect of using different vendor's DECT systems, although investigated in multiple phantom studies, should be explored in a clinical setting.

In conclusion, this proof of principle study shows that DECT iodine concentration quantified from rest-stress imaging has the potential to distinguish between normal, ischemic, and infarcted myocardium.

REFERENCES

1. Jin KN, De Cecco CN, Caruso D, Tesche C, Spandorfer A, Varga-Szemes A, et al. Myocardial perfusion imaging with dual energy CT. Eur J Radiol [Internet]. 2016;85(10):1914–21. Available from: http://dx.doi.org/10.1016/j.ejrad.2016.06.023
2. Schwarz F, Ruzsics B, Schoepf UJ, Bastarrika G, Chiaramida SA, Abro JA, et al. Dual-energy CT of the heart-Principles and protocols. Eur J Radiol. 2008;68(3):423–33.
3. Koonce JD, Vliegenthart R, Schoepf UJ, Schmidt B, Wahlquist AE, Nietert PJ, et al. Protocols : Validation in a Phantom Model Phantom setup. 2014;24(2):512–8.
4. Vliegenthart R, Henzler T, Moscariello A, Ruzsics B, Bastarrika G, Oudkerk M, et al. CT of coronary heart disease: Part 1, CT of myocardial infarction, ischemia, and viability. Am J Roentgenol. 2012;198(3):531–47.
5. Ruzsics B, Lee H, Powers ER, Flohr TG, Costello P, Schoepf UJ. Myocardial ischemia diagnosed by dual-energy computed tomography: Correlation with single-photon emission computed tomography. Circulation. 2008;117(9):1244–5.
6. Nakahara, T., Toyama, T., Jinzaki, M., Seki, R., Saito, Y., Higuchi, T., Yamada, M., Arai, M., Tsushima, Y., Kuribayashi, S., Kurabayashi M. Quantitative Analysis of Iodine Image of Dual-energy Computed Tomography at Rest: Comparison With 99mTc-Tetrofosmin Stress-rest Single-photon Emission Computed Tomography Myocardial Perfusion Imaging as the Reference Standard. J Thorac Imaging. 2018;33(2):97–104.
7. Pelgrim GJ, van Hamersvelt RW, Willemink MJ, Schmidt BT, Flohr T, Schilham A, et al. Accuracy of iodine quantification using dual energy CT in latest generation dual source and dual layer CT. Eur Radiol. 2017;1–9.
8. Lenga L, Albrecht MH, Othman AE, Martin SS, Leithner D, D'Angelo T AC, Scholtz JE, De Cecco CN, Schoepf UJ, Vogl TJ WJ. Monoenergetic Dual-energy Computed Tomographic Imaging: Cardiothoracic Applications. J Thorac Imaging. 2017;32(3):151–8.
9. Tabari A, Lo Gullo R, Murugan V, Otrakji A, Digumarthy S KM. Recent Advances in Computed Tomographic Technology: Cardiopulmonary Imaging Applications. J Thorac Imaging. 2017;32(2):89–100.
10. Ko SM, Choi JW, Song MG, Shin JK, Chee HK, Chung HW, et al. Myocardial perfusion imaging using adenosine-induced stress dual-energy computed tomography of the heart: comparison with cardiac magnetic resonance imaging and conventional coronary angiography. Eur Radiol. 2011 Jan;21(1):26–35.
11. Ruzsics B, Schwarz F, Schoepf UJ, Lee YS, Bastarrika G, Chiaramida SA, et al. Comparison of Dual-Energy Computed Tomography of the Heart With Single Photon Emission Computed Tomography for Assessment of Coronary Artery Stenosis and of the Myocardial Blood Supply. Am J Cardiol [Internet]. 2009;104(3):318–26. Available from: http://linkinghub.elsevier.com/retrieve/pii/S0002914909008133
12. Ko SM, Park JH, Hwang HK, Song MG. Direct comparison of stress- and rest-dual-energy computed tomography for detection of myocardial perfusion defect. Int J Cardiovasc Imaging [Internet]. 2014;30(S1):41–53. Available from: http://link.springer.com/10.1007/s10554-014-0410-3
13. Delgado Sanchez-Gracian C, Oca Pernas R, Trinidad Lopez C, Santos Armentia E, Vaamonde Liste A, Vazquez Caamano M, et al. Quantitative myocardial perfusion with stress dual-energy CT: iodine concentration differences between normal and ischemic or necrotic myocardium. Initial experience. Eur Radiol [Internet]. 2016;26(9):3199–207. Available from: http://dx.doi.org/10.1007/s00330-015-4128-y

14. Danad I, Raijmakers PG, Driessen RS, Leipsic J, Raju R, Naoum C, et al. Comparison of coronary CT angiography, SPECT, PET, and hybrid imaging for diagnosis of ischemic heart disease determined by fractional flow reserve. JAMA Cardiol. 2017;2(10):1100–7.

15. Meinel FG, De Cecco CN, Schoepf UJ, Nance JW, Silverman JR, Flowers B a, et al. First-Arterial-Pass Dual-Energy CT for Assessment of Myocardial Blood Supply: Do We Need Rest, Stress, and Delayed Acquisition? Comparison with SPECT. Radiology [Internet]. 2013;270(3):131183. Available from: http://www.ncbi.nlm.nih.gov/pubmed/24475833

16. Achenbach S. Computed Tomography Coronary Angiography. J Am Coll Cardiol. 2006;48(10):1919–28.

17. Bamberg F, Hinkel R, Schwarz F, Sandner TA, Baloch E, Marcus R, et al. Accuracy of Dynamic Computed Tomography Adenosine Stress Myocardial Perfusion Imaging in Estimating Myocardial Blood Flow at Various Degrees of Coronary Artery Stenosis Using a Porcine Animal Model. Invest Radiol. 2012;47(1):71–7.

18. Jaarsma C, Leiner T, Bekkers SC, Crijns HJ, Wildberger JE, Nagel E, et al. Diagnostic Performance of Noninvasive Myocardial Perfusion Imaging Using Single-Photon Emission Computed Tomography, Cardiac Magnetic Resonance, and Positron Emission Tomography Imaging for the Detection of Obstructive Coronary Artery Disease. J Am Coll Cardiol [Internet]. 2012;59(19):1719–28. Available from: http://www.ncbi.nlm.nih.gov/entrez/query.fcgi?cmd=Retrieve&db=PubMed&dopt=Citation&list_uids=22554604

19. Kostkiewicz M. Myocardial perfusion imaging in coronary artery disease. Cor Vasa [Internet]. 2015;57(6):e446–52. Available from: http://dx.doi.org/10.1016/j.crvasa.2015.09.010

20. Liu A, Wijesurendra RS, Francis JM, Robson MD, Neubauer S, Piechnik SK, et al. Adenosine Stress and Rest T1 Mapping Can Differentiate Between Ischemic, lnfarcted, Remote, and Normal Myocardium Without the Need for Gadolinium Contrast Agents. JACC Cardiovasc Imaging [Internet]. 2016 Jan;9(1, SI):27–36. Available from: http://www.embase.com/search/results?subaction=viewrecord&from=export&id=L607256480

21. Uren NG, Marraccini P, Gistri R, de Silva R, Camici PG. Altered coronary vasodilator reserve and metabolism in myocardium subtended by normal arteries in patients with coronary artery disease. J Am Coll Cardiol [Internet]. 1993;22(3):650–8. Available from: http://dx.doi.org/10.1016/0735-1097(93)90172-W

22. Kaufmann PA, Camici PG. Myocardial Blood Flow Measurement by PET: Technical Aspects and Clinical Applications. J Nucl Med. 2005;46(1):75–88.

23. Salerno M, Beller GA. Noninvasive assessment of myocardial perfusion. Circ Cardiovasc Imaging. 2009;2(5):412–24.